J. Membrane Biol. 41, 167–187 (1978)

Spectral Analysis of Current Noise Generated by Carrier-Mediated Ion Transport

H.-A. Kolb and P. Läuger

Department of Biology, University of Konstanz, D-775 Konstanz, Germany

Received 19 December 1977

Summary. It is shown that valinomycin-mediated alkali ion transport is associated with a characteristic type of current noise. The spectral intensity of the noise which is measured under equilibrium conditions, i.e., at zero net current, is frequency independent ("white") both at high and at low frequencies. The transition between the low- and the high-frequency limit occurs in a frequency range which is related to the characteristic relaxation time constants of the transport system. This behavior is predicted from the carrier transport model on the basis of Nyquist's theorem.

From the current and voltage fluctuations which are associated with the transport of ions through biological membranes, information on the transport mechanism may be obtained (Verveen & DeFelice, 1974; Conti & Wanke, 1975; DeFelice, 1977; Neher & Stevens, 1977). So far, most noise studies with biological membranes have been devoted to the analysis of opening-closing processes of ion channels in excitable membranes. It is well known that this type of noise which results from transitions between different conductance states of a channel is characterized by a Lorentzian spectrum with a frequency-independent limit at low frequencies and a decline toward high frequencies. A completely different type of noise has to be expected for carrier-mediated ion transport. In this case noise results from random fluctuations in the number of charged carrier molecules crossing the membrane dielectric in a given time interval. Although attempts have been made to study noise originating from an active ion transport system (Segal, 1972; Fishman & Dorset, 1973; Segal, 1973), unequivocal evidence for noise associated with carrier-mediated ion transport has not been obtained so far.

In this paper we describe noise studies with lipid bilayer membranes in the presence of the cation-carrier valinomycin. Valinomycin is a hydrophobic depsipeptide which is known to form complexes with alkali

0022-2631/78/0041-0167 $04.20

ions such as K^+ or Rb^+; the complex which is formed at one membrane-solution interface is able to move across the membrane dielectric to the opposite interface where the ion is released to the aqueous solution (for a review of the literature, *see* Szabo *et al.*, 1973). In the experiments described below the current noise of a valinomycin-doped black lipid film was measured at equilibrium, i.e., with external solutions of identical composition and at zero voltage. Under these conditions the average membrane current vanishes, but at any moment the instantaneous current differs from zero. This current, which fluctuates around zero, arises from random variations in the number of charged ion-carrier complexes crossing the membrane from right to left and from left to right. In this respect the noise from the carrier system is similar to the recently described current noise of lipid bilayers in the presence of hydrophobic ions (Kolb & Läuger, 1977; Szabo, 1977). The main difference between both transport systems lies in the fact that the exchange of hydrophobic ions between interface and aqueous solution is usually very slow (much slower than the rate of crossing the membrane), whereas the dissociation rate of the ion-carrier complex in the interface may be of the same order of magnitude as (or even larger than) the translocation rate across the membrane. This means that the current-noise spectrum of the carrier system should be "white" (i.e., frequency independent) both at the low- and high-frequency end of the spectrum. In the following we show that the valinomycin/Rb^+ system yields a noise spectrum which has the theoretically expected shape.

Theory

For the analysis of noise from the ion carrier system we use a transport model which has been previously proposed on the basis of the steady-state and transient behavior of the carrier (Läuger & Stark, 1970; Stark & Benz, 1971; Stark, Ketterer, Benz and Läuger, 1971). According to this model, the transfer of an ion across the membrane occurs in four distinct steps (Fig. 1): (i) formation of a complex between ion M^+ and carrier S in the membrane-solution interface (rate constants k_R), (ii) translocation of MS^+ across the membrane (rate constant k'_{MS} and k''_{MS}), (iii) dissociation of MS^+ and release of M^+ to the solution (rate constant k_D), (iv) back transport of the free carrier S (rate constant k_S; for a symmetrical membrane, the rate constants for the translocation of S are identical in both directions.) Neglecting the slight field-dependence of k_R

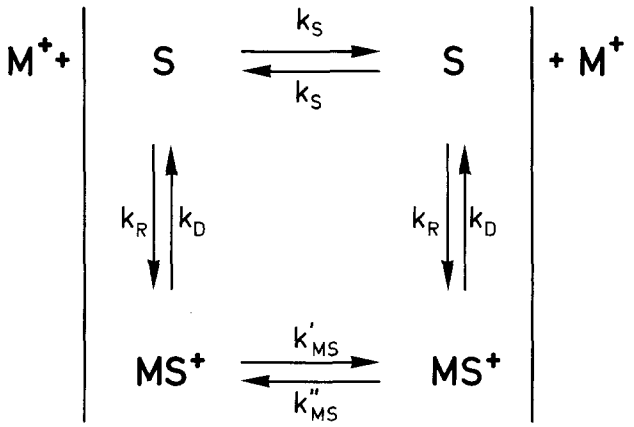

Fig. 1. Transport model of the ion-carrier system

and k_D (Stark & Benz, 1971; Eisenman, Krasne & Ciani, 1975: Hladky, 1975; Feldberg & Nakadomari, 1977), we assume that k'_{MS} and k''_{MS} are the only rate constants which depend on the external voltage. This means that the equilibrium constant for complexation:

$$K_h = \frac{k_R}{k_D} = \frac{N_{MS}}{N_S c_M} \tag{1}$$

is independent of external voltage; N_{MS} and N_S are the average interfacial concentrations (expressed in cm^{-2}) of MS^+ and S at equilibrium referred to one interface, and c_M is the concentration of M^+ in water. We further assume that the total carrier concentration N in the membrane:

$$N = N'_S + N''_S + N'_{MS} + N''_{MS} \tag{2}$$

is time-independent (N'_S, N''_S, N'_{MS}, N''_{MS} are the interfacial concentrations at the left (′) and right (″) interface at any given moment). This assumption is justified within the time scale of the noise experiments (milliseconds), as the exchange of carrier molecules between membrane and water is a very slow process (Stark & Benz, 1971).

According to Nyquist's theorem (Nyquist, 1928; Callen & Welton, 1951; Callen & Greene, 1952; Kubo, 1957), the spectral intensity $S_I(\omega)$ of current noise at equilibrium is related to the complex admittance $Y(\omega)$ of the transport system ($1/Y$ is the impedance):

$$S_I(\omega) = 4kT \cdot \mathrm{Re}[Y(\omega)]. \tag{3}$$

k is the Boltzmann constant, T the absolute temperature, ω the angular frequency and Re means "real part of." On the basis of the transport model described above, the admittance of a membrane for small signals in the presence of the carrier system is easily calculated (*see* Appendix *A*). The result reads (e_0 is the elementary charge and A_m the membrane area):

$$S_I(\omega)=4e_0^2A_mN_{MS}k_{MS}\left(1-\frac{\alpha_1}{1+\omega^2\tau_1^2}-\frac{\alpha_2}{1+\omega^2\tau_2^2}\right) \tag{4}$$

$$\alpha_1=\frac{k_{MS}}{\sqrt{a}}\cdot\frac{\sqrt{a}-P}{\sqrt{a}+Q};\qquad \alpha_2=\frac{k_{MS}}{\sqrt{a}}\cdot\frac{P+\sqrt{a}}{Q-\sqrt{a}} \tag{5}$$

$$\tau_1=\frac{1}{Q+\sqrt{a}};\qquad \tau_2=\frac{1}{Q-\sqrt{a}} \tag{6}$$

$$P=\frac{1}{2}(c_Mk_R-k_D+2k_S-2k_{MS}) \tag{7}$$

$$Q=\frac{1}{2}(c_Mk_R+k_D+2k_S+2k_{MS}) \tag{8}$$

$$a=P^2+c_Mk_Rk_D. \tag{9}$$

It is seen from Eq. (4) that the spectral intensity $S_I(\omega)$ approaches frequency-independent ("white" noise) limits both at low and high frequencies ω. The low-frequency limit may be written in the form [using Eqs. (5)–(7)]

$$S_I(0)=4kTA_m\lambda_{0\infty} \tag{10}$$

$$\lambda_{0\infty}=\frac{e_0^2}{kT}\cdot\frac{k_{MS}N_{MS}}{1+\frac{2k_{MS}}{k_D}+\frac{c_Mk_Rk_{MS}}{k_Dk_S}}. \tag{11}$$

$\lambda_{0\infty}$ is the ohmic steady-state conductance of the membrane per unit area (Stark *et al.*, 1971). The high-frequency limit is given by

$$S_I(\infty)=4e_0^2A_mk_{MS}N_{MS}=4kTA_m\lambda_{00} \tag{12}$$

where $\lambda_{00}=(e_0^2/kT)k_{MS}N_{MS}$ is the initial ohmic conductance which is observed at time zero after a voltage jump (Stark *et al.*, 1971).

A similar expression for $S_I(\infty)$ has been recently derived for a membrane doped with hydrophobic ions (Kolb & Läuger, 1977). Between the low- and high-frequency limit two dispersion regions occur at

frequencies $\omega_1 = 1/\tau_1$ and $\omega_2 = 1/\tau_2$. The time constants τ_1 and τ_2 Eq. (6) are identical with the relaxation times of the carrier system in a voltage-jump experiment (Stark *et al.*, 1971).

As the theoretical expression for the spectral intensity [Eqs. (4)–(9)] is somewhat complicated, it is instructive to consider a special case in which the spectral parameters can be expressed directly in terms of the rate constants. For this purpose we assume that the translocation rate constants of the loaded and the unloaded carrier are equal ($k_{MS} = k_S \equiv k_t$); the expressions for the time constant τ_1, τ_2 and the "amplitudes" α_1, α_2 then assume the simple form:

$$\tau_1 = \frac{1}{c_M k_R + k_D + 2k_t}, \qquad \tau_2 = \frac{1}{2k_t} \tag{13}$$

$$\alpha_1 = \frac{2k_D k_t}{(c_M k_R + k_D)(c_M k_R + k_D + 2k_t)}, \qquad \alpha_2 = \frac{c_M k_R}{c_M k_R + k_D}. \tag{14}$$

If we further assume that the translocation process is rate limiting ($c_M k_R$, $k_D \gg k_t$), then

$$\tau_1 \approx \frac{1}{c_M k_R + k_D} \ll \tau_2 = \frac{1}{2k_t} \tag{15}$$

$$\alpha_1 \approx \frac{2k_t/k_D}{(1 + c_M k_R/k_D)^2} \ll 1. \tag{16}$$

This means that one time constant becomes much shorter than the other and that the corresponding amplitude α_1 vanishes. If we assume, on the other hand, that the surface reaction is rate limiting ($c_M k_R, k_D \ll k_t$), then

$$\tau_1 \approx \tau_2 = \frac{1}{2k_t} \tag{17}$$

$$\alpha_1 \approx \frac{k_D}{c_M k_R + k_D}, \qquad \alpha_2 = \frac{k_R}{c_M k_R + k_D}. \tag{18}$$

In this case both time constants become identical so that again only a single dispersion is observed.

Materials and Methods

Optically black lipid bilayer membranes were formed in the usual way (Läuger *et al.*, 1967) from a 2% (w/v) solution of monoglycerides (Nu Check Prep., Elysian, Minn.) with C_{18} to C_{22} cis-mono-unsaturated fatty acid chains (monoolein, monoeicosenoin, mo-

noerucin) in *n*-decane (Merck, standard for gas chromatography). The lipids contained about 98% of the 1-isomer and gave a single spot in a thin-layer chromatogram. The circular hole in the Teflon wall between the two thermostated aqueous compartments had a diameter of about 0.25 mm. The area of the black membrane was determined with a calibrated scale in the ocular of a microscope. The aqueous phase contained 1 M RbCl or 1 M LiCl (Merck, analytical grade) and 10^{-7} M valinomycin (Calbiochem, San Diego, Calif.) dissolved in twice-distilled water. The aqueous solutions were unbuffered and had a pH of about 6. Prior to membrane formation, the Teflon cell with inserted Ag/AgCl electrodes were incubated for about 3 hr with the aqueous solution at room temperature. The measurements were started 50–60 min after the membrane had turned completely black. The spectral intensity of the current noise of the black film was measured at zero voltage, as described previously (Kolb & Läuger, 1977). The feedback resistance R_f of the preamplifier (Analog Devices Model 52 K) was set to 20 MΩ, if not stated otherwise. Furthermore, a constant feedback capacitance C_f of 1 pF was used. The output of the preamplifier was fed into the main amplifier (Princeton Applied Research Model 113) which was used in the ac-coupled mode with a lower cut-off frequency of 1 Hz and a higher cut-off frequency of 300 kHz (the upper frequency limit of the measurement is then mainly determined by the feedback circuit of the preamplifier). S_I of the current noise was processed on-line with a Honeywell-Saicor 52B real-time spectrum analyzer. The recorded spectrum usually was an average of 512 summations.

In addition to the noise from the source under study (the membrane cell or a model circuit), noise is generated by the amplifying system itself, in particular by the preamplifier. The intrinsic noise of the preamplifier may be described to a first approximation by introducing at the input of the amplifier a voltage-noise source of spectral intensity S_v and an independent current-noise source of spectral intensity S_i (Poussart, 1971). If the input of the preamplifier is connected to a source of impedance Z, the spectral intensity $S_{I,b}$ of the background current noise generated by the preamplifier is given by (Poussart, 1971; Kolb & Läuger, 1977):

$$S_{I,b} = S_i + S_v \left\{ \frac{1}{R_f^2} + \frac{1}{|Z|^2} \left[1 + 2 \frac{\mathrm{Re}(Z)}{R_f} \right] \right\} + \frac{4kT}{R_f}. \tag{19}$$

R_f is the feedback resistance of the preamplifier. The total spectral intensity $S_{I,t}$ is then the sum of the noise contribution of the source, $S_{I,s}$ and of the preamplifier, $S_{I,b}$:

$$S_{I,t} = S_{I,s} + S_{I,b}. \tag{20}$$

The filter function of the amplifying system is described by the 3-db attenuation frequencies f_1 and f_2; $f_1 = 1$ Hz is the lower cut-off frequency of the main amplifier and $f_2 = 1/2\pi R_f C_f$ is the higher cut-off frequency (C_f is the feed-back capacitance) of the preamplifier. The influence of this filtering on the measured noise signal may be described by multiplying the spectral intensity by the filter transfer function $|g(f)|^2$ defined by the relation ($f = \omega/2\pi$ is the frequency):

$$|g(f)|^2 = \frac{f_2^2 f^2}{(f_1^2 + f^2)(f_2^2 + f^2)}. \tag{21}$$

In order to test the performance of the amplifying system and the spectrum analyzer, the membrane cell was replaced by a model circuit yielding a similar noise spectrum as the expected noise spectrum from the carrier system. The model circuit (Fig. 2) consisted of a series combination of a resistance R_A and a capacitance C_A in parallel with a resistance R_B. A further capacitance C_m was added in parallel to R_B in order to simulate

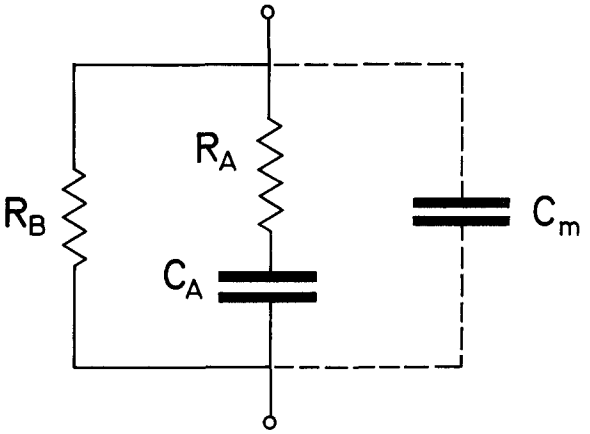

Fig. 2. Model circuit used for a test of the electronic set-up

the influence of the membrane capacitance (*see below*). According to Nyquist's theorem [Eq. (3)], the spectral intensity of the model circuit may be calculated from the circuit admittance to be

$$S_{I,s}(\omega)=4kT\left(\frac{1}{R_B}+\frac{1}{R_A}\cdot\frac{\omega^2\tau_A^2}{1+\omega^2\tau_A^2}\right) \tag{22}$$

$$\tau_A=R_A C_A.$$

It is seen from Eq. (22) that the current noise spectrum $S_{I,s}(\omega)$ of the model circuit is independent of C_m. $S_{I,s}(\omega)$ is "white" both at low and high frequency and shows a single dispersion near $\omega=1/\tau_A$ (instead of the two dispersions to be expected for the carrier system).

Results from experiments with model circuits are represented in Figs. 3 and 4. In Fig. 3 the influence of the "membrane capacitance" C_m (Fig. 2) is shown. The measured spectral intensity corresponds to the quantity $[S_{I,s}(f)+S_{I,b}(f)]\cdot|g(f)|^2$ (dotted lines in Fig. 3) which has been calculated according to Eqs. (19), (21), and (22) for different values of C_m using the values of $S_i(f)$ and $S_v(f)$ given in the specifications of the Analog Devices 52 K preamplifier. For higher C_m values the measured spectral intensity strongly increases above 2 kHz. This deviation is caused presumably by an increase of the voltage noise of the amplifying system for frequencies above 2 kHz which is transformed into current noise by the capacitance C_m. For the calculation of $S_{I,b}$ [Eq. (19)] a frequency dependency of S_v was not taken into account. The dashed line is the theoretical spectrum of the model circuit [$S_{I,s}(f)$ in Eq. (20)] which has been calculated from Eq. (22). It is seen that the experimental spectral intensity is close to the theoretical spectrum only at low values of C_m.

The influence of the feedback resistance R_f is represented in Fig. 4. In these experiments the same model circuit has been used as in Fig. 3, but at a constant value of $C_m=56$pF. For $R_f=20\,\mathrm{M\Omega}$ the spectrum shows little deviation from the theoretically expected behavior (dashed line) in the frequency range up to 5 kHz (as already shown in Fig. 3), but for $R_f=50\,\mathrm{M\Omega}$ (and larger values) $S_I(f)$ declines toward high frequencies. This decrease of the spectral intensity results mainly from the filter effect of the feedback circuit; for instance, at $R_f=50\,\mathrm{M\Omega}$ and $C_f=1$ pF the upper cut-off frequency is $f_2=1/2\pi R_f C_f=3.2$ kHz.

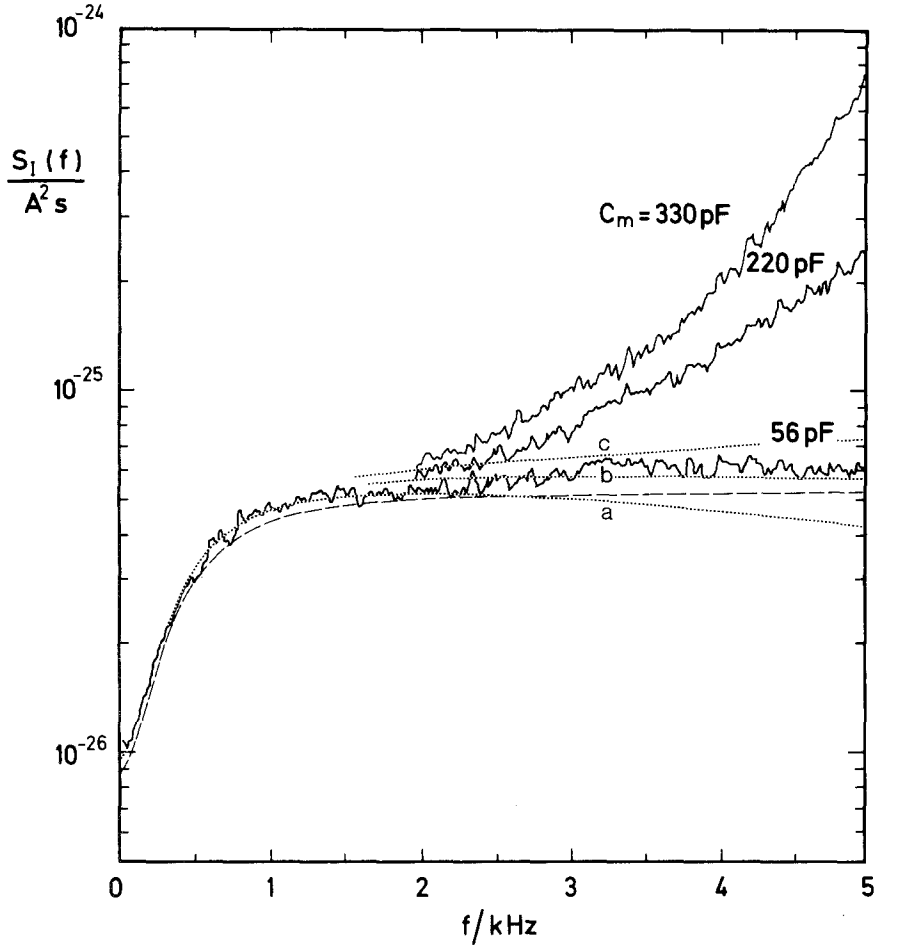

Fig. 3. Spectral intensity $S_I(f)$ of current noise at zero voltage from the model circuit shown in Fig. 2 ($R_A = 0.36\,\mathrm{M}\Omega$, $C_A = 820$ pF, $R_B = 1.82\,\mathrm{M}\Omega$) for different values of the capacitance C_m. The feedback resistance was $R_f = 20\,\mathrm{M}\Omega$. The dashed line is the theoretical spectrum $S_{I,s}(f)$ calculated from Eq. (22). The dotted lines represent the function $[S_{I,s}(f) + S_{I,b}(f)] \cdot |g(f)|^2$ which has been calculated according to Eqs. (19), (21) and (22) for various C_m values: 56 pF (curve *a*), 220 pF (curve *b*), 330 pF (curve *c*), using the values of $S_i(f)$ and $S_v(f)$ given in the specifications of the Analog Devices 52 K preamplifier

From these considerations it is clear that a proper choice of C_m and R_f has to represent a compromise between high bandwidth and low-noise performance of the measuring circuit. Making the membrane area A_m small (and therefore also the membrane capacitance C_m) has the desirable effect of reducing the background noise created by the preamplifier (Fig. 3). At low A_m, however, the membrane resistance (corresponding to R_B in Fig. 2) becomes large which requires a larger value of R_f (otherwise the current noise of the feedback circuit would become predominant at low frequencies). An increase of R_f in turn reduces the bandwidth of the feedback circuit. In the membrane experiments the capacitance C_m was kept below 100 pF which corresponds, with a specific membrane

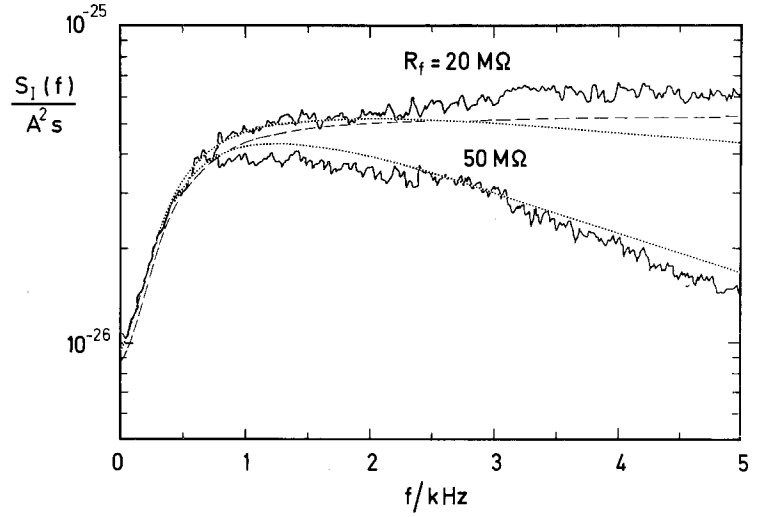

Fig. 4. Spectral intensity of current noise measured under the same conditions as in Fig. 3, but at a fixed value of $C_m = 56$ pF and two different values of the feedback resistance R_f. (The curve for $R_f = 20\,M\Omega$ is identical with the curve labeled "56 pF" in Fig. 3). The dashed line is the theoretical spectrum $S_{I,s}(f)$ calculated from Eq. (22). The dotted lines represent the function $[S_{I,s}(f) + S_{I,b}(f)] \cdot |g(f)|^2$ calculated for the different values of R_f. *See* Fig. 3 for further explanations

capacitance of 318 nF cm^{-2} (Benz *et al.*, 1975), to a membrane area of less than 3×10^{-4} cm^2. In this way distortions of the spectra were usually negligible below 2 kHz; in most cases only this lower frequency range was used for the determination of kinetic parameters. Only for the measurements at higher temperatures did corrections for the limited bandwidth and the background noise have to be introduced (*compare* Table 1).

Pairs of Ag/AgCl electrodes were selected with asymmetry potentials of less than 0.2 mV. It was checked that the spectral density of current noise was independent of applied voltage in the range of 0–5 mV. For this reason the influence of electrode polarization could be neglected. In order to exclude the possibility that noise from the electrodes interfered with the measurements, test experiment were carried out in which the cell with membrane and electrodes was connected in the usual way to the preamplifier; valinomycin, however, was omitted and the valinomycin-induced conductance was simulated by a parallel resistor R_m of suitable size. In this case only the noise expected from R_m, C_m, and the amplifier characteristics was observed (*see below*).

Results

A current-noise spectrum recorded under equilibrium conditions from a membrane in the presence of 10^{-7} M valinomycin and 1 M Rb^+ is represented in Fig. 5 (curve *a*). The spectrum shows a frequency-independent part at high frequencies and a decline to a constant value at low frequencies (the fact that $S_I(f)$ approaches a constant value at low f is

Table 1. Temperature dependence of the spectral parameters of current noise in the presence of 10^{-7} M valinomycin and 1 M Rb^+

T °C	$S_I(0)$ 10^{-27} A^2 s	$\frac{(\lambda_{0,\infty})_{noise}}{(\lambda_{0,\infty})_{I/V}}$	$S_I(\infty)$ 10^{-26} A^2 s	f_c kHz	$f_{c,korr}$ kHz
Monoolein (18:1)					
2	13.0±2.5	1.10±0.11	10.6±2.2	2.3 ±0.5	2.6 ±0.4
10	14.1±2.6	1.09±0.12	11.8±3.1	9.8 ±2.1	10.3 ±2.1
Monoeicosenoin (20:1)					
2	12.4±1.6	1.03±0.04	8.6±1.4	0.82+0.11	0.85±0.10
10	12.2±0.1	1.10±0.11	9.5±1.8	2.2 ±0.4	2.6 ±0.4
Monoerucin (22:1)					
2	8.3±1.3	1.05±0.07	5.4±0.8	0.55±0.07	0.56±0.07
10	8.4±1.1	1.07±0.04	6.0±1.1	1.7 ±0.5	1.9 ±0.4
20	9.3±1.8	1.15±0.2	6.2±2.0	7.4 ±2.0	8.1 ±2.5
30	9.6±1.6	1.2 ±0.3	–	18[b]	24[b]

[a] Mean values obtained from 10 different membranes for each temperature are given together with the standard deviations. $S_I(0)$ and $S_I(\infty)$ are the limiting values of the spectral intensity at low and high frequency, respectively. Both quantities have been taken from least-squares fits of Eq. (23) to the recorded spectra. The experimental spectra have been corrected at frequencies above 2 kHz for the background noise and the influence of the filter function (*see Materials and Methods*); $(\lambda_{0\infty})_{noise}$ is the ohmic steady-state conductance of the membrane calculated from $S_I(0)$ according to Eq. (10), $(\lambda_{0\infty})_{I/V}$ the conductance obtained directly by measuring the mean steady-state current at a voltage of 10 mV. f_c is the corner frequency [Eq. (23)] evaluated from the experimental spectra, $f_{c,korr}$ the corner frequency which is obtained after correction of the spectra (*see above*). The data are normalized to an area of $A_m = 1.5 \times 10^{-4}$ cm^2.

[b] Estimated values from $S_I(f)$ measured for $f < 10$ kHz.

more clearly seen from a plot on a logarithmic frequency scale such as Fig. 6). The experimental result is thus consistent with the expectation that the spectrum should be white both at low and at high frequencies. A closer analysis shows that the transition between the low- and the high-frequency value of $S_I(f)$ can be described (within the experimental accuracy) by a single dispersion, i.e., by an equation of the form

$$S_I(f) = S_I(0) + [S_I(\infty) - S_I(0)] \frac{f^2}{f_c^2 + f^2} \tag{23}$$

where f_c is the "corner frequency", i.e., the midpoint in the transition between $S_I(0)$ and $S_I(\infty)$. A fit of Eq. (23) to the experimental spectrum is represented by curve *b* in Fig. 5. For this fit only the measured values below 2 kHz have been used; the slight rise of the experimental spectrum at higher frequencies is also seen with dummy circuits of the type shown in Fig. 2 and is, therefore, probably not related to the carrier system.

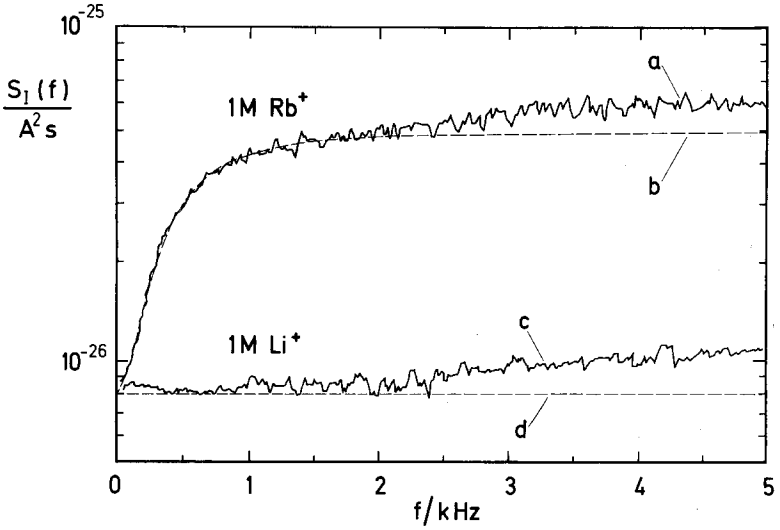

Fig. 5. Spectral intensity of current noise from a lipid bilayer membrane in the presence of 10^{-7} M valinomycin under equilibrium conditions; $T=2$ °C, membrane area $A_m=1.6$ 10^{-4} cm^2 and membrane capacitance $C_m\cong 51$ pF. Curve *a*: 1 M RbCl on both sides. Curve *b*: fit of Eq. (23) to curve *a* with $f_c=510$ Hz (for the fitting precedure only the values below 2 kHz have been used). Curve *c*: 1 M LiCl on both sides with an external resistor $R_m=360$ kΩ added in parallel to the membrane to give the same stationary conductance as under the conditions of curve *a*. Curve *d*: thermal noise spectrum calculated according to $S_I=4kT/R_m$

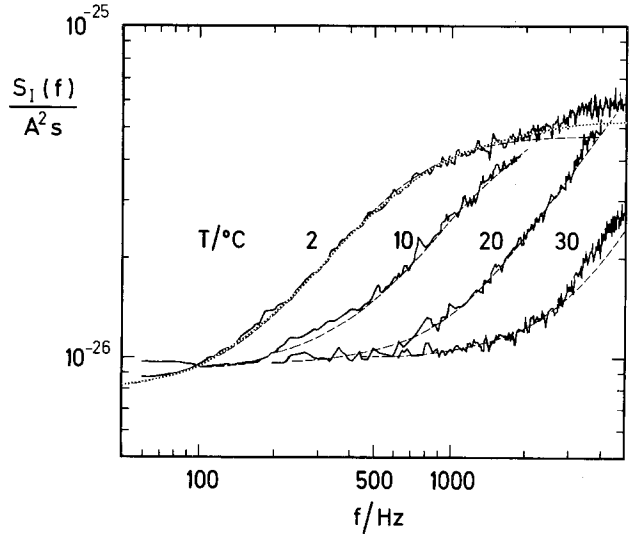

Fig. 6. Temperature dependence of the spectral intensity of current noise. The aqueous phase contained 10^{-7} M valinomycin and 1 M RbCl. All records have been obtained with one and the same membrane ($A_m=1.6\times10^{-4}$ cm^2). The dashed lines are fits of Eq. (23) to the experimental spectra. The dotted line represents a fit of Eq. (4) to the spectrum at 2 °C using the following parameter values: $k_R=1.7\times10^3$ M^{-1} s^{-1}, $k_D=1\times10^3$ s^{-1}, $k_S=1\times10^3$ s^{-1}, $k_{MS}=1.7\times10^3$ s^{-1}, $N_{MS}=3.5$ pmol cm^{-2}

Curve *c* of Fig. 5 represents a control experiment in which Rb^+ has been replaced by Li^+; Li^+ is not transported to any appreciable extent by valinomycin (Benz, 1972). In this experiment an external resistor of magnitude R_m has been added in parallel to the membrane in order to give the same stationary conductance as with 1 M Rb^+. In this case only white noise is observed over the whole frequency range; the spectral intensity closely agrees with the thermal noise level calculated from R_m according to the Nyquist relation (curve *d*). Furthermore, with R_m present, the observed spectrum is unaffected when the valinomycin concentration is varied or when valinomycin is completely omitted.

The experimental result which is contained in Fig. 5 and Eq. (23) may be compared with the noise spectrum predicted from the theoretical model [Eq. (4)]. Whereas theory predicts, in general, two dispersions, only one dispersion has been found experimentally. A situation where only one dispersion is observed can arise in different ways. If in Eq. (6) Q becomes much larger than $\sqrt{a}$, the two time constants τ_1 and τ_2 become nearly equal so that (within the experimental accuracy) both dispersions fuse into a single dispersion region; or τ_1 and τ_2 may be sufficiently different, but one of the "amplitudes", α_1 or α_2 in Eq. (4), becomes much larger than the other. Such examples have already been discussed in the theoretical section for the special case $k_S = k_{MS}$. The comparison with voltage-jump relaxation data (*see below*) suggests that in the system studied here both time constants τ_1 and τ_2 have similar values.

Fig. 6 shows the temperature dependence of the spectral intensity in the range between 2 and 30 °C. At all temperatures the observed spectrum could be approximately fitted by a function of the form of Eq. (23) (dashed lines in Fig. 6). Again, at higher frequencies deviations of the spectral shape given by Eq. (23) occur, which result from excess noise produced by the preamplifier. The limiting spectral intensity at low frequency, $S_I(0)$, is remarkably insensitive to temperature, as Fig. 6 shows. According to Eqs. (10) and (11), $S_I(0)$ is proportional to the ohmic steady-state conductance $\lambda_{0\infty}$ and thus depends on the rate constants of the carrier system (k_R, k_D, k_S and k_{MS}), as well as on the concentration N_{MS} of the loaded carrier in the membrane. The finding that $S_I(0)$ is virtually insensitive to a variation of temperature is consistent with the previously observed temperature-independent behavior of valinomycin-mediated potassium conductance (Stark *et al.*, 1972). Those findings have been explained by the fact that, although the rate constants increase with temperature, this increase is nearly compensated (in terms of steady-state conductance) by a decrease of the partition coefficient of the carrier, i.e.,

by a decrease of valinomycin concentration in the membrane (Benz *et al.*, 1973). According to this explanation only a small temperature dependence of $S_I(\infty)$ should be observed, too, which is confirmed by the measurements (Table 1).

In contrast to $S_I(0)$ and $S_I(\infty)$, the corner frequency f_c strongly depends on temperature (Fig. 6 and Table 1). Between 2 and 30 °C, f_c increases by a factor of about 30.

According to Eq. (10) the limiting spectral intensity at low frequency, $S_I(0)$, is related to the ohmic steady-state conductance $\lambda_{0\infty}$. The $\lambda_{0\infty}$ values which are calculated from $S_I(0)$ may be compared with the steady-state conductance obtained directly from a measurement of the mean steady-state current at a given small voltage. As seen from Table 1, the ratio of both quantities is close to unity at all temperatures.

The experimental values of $S_I(f)$ may be used to evaluate the five parameters of the carrier model, k_R, k_D, k_S, k_{MS} and N_{MS}, provided that the spectrum has been measured with sufficient accuracy over a sufficiently broad frequency range (expressions relating the rate constants and N_{MS} to the spectral parameters are given in Appendix *B*). In the system studied here, however, this procedure is not feasible, because only one dispersion could be resolved at the given experimental accuracy. We therefore restrict ourselves to show that the observed spectra are consistent with physically reasonable values of the model parameters. In Fig. 6 the dotted line represents a fit of Eq. (4) to the experimental spectrum at 2 °C, using the following values: $k_R = 1.7 \times 10^3\,\mathrm{M^{-1}\,s^{-1}}$ $k_D = 1 \times 10^3\,\mathrm{s^{-1}}$, $k_S = 1 \times 10^3\,\mathrm{s^{-1}}$, $k_{MS} = 1.7 \times 10^3\,\mathrm{s^{-1}}$, $N_{MS} = 3.5\,\mathrm{pmol\,cm^{-2}}$.

In order to compare the fitted values of the model parameters for observed spectral intensities with available voltage-jump and charge-pulse relaxation data (Knoll & Stark, 1975; Benz & Läuger, 1976) the spectral intensity of a monoolein/*n*-decane membrane was measured at 10 °C in the presence of 10^{-7} M valinomycin and 1 M RbCl in the aqueous solution. For this system the following set of parameters can be used for a fit to the experimental spectrum (values determined from the voltage-jump and charge-pulse relaxation data are given in parenthesis, respectively)

$$k_R = 8 \times 10^4\,\mathrm{M^{-1}\,s^{-1}} \quad (8.1 \times 10^4\,\mathrm{M^{-1}\,s^{-1}},\ 11 \times 10^4\,\mathrm{M^{-1}\,s^{-1}}),$$
$$k_D = 1.2 \times 10^4\,\mathrm{s^{-1}} \quad (1.7 \times 10^4\,\mathrm{s^{-1}},\ 3.7 \times 10^4\,\mathrm{s^{-1}}),$$
$$k_S = 1.0 \times 10^4\,\mathrm{s^{-1}} \quad (1.0 \times 10^4\,\mathrm{s^{-1}},\ 0.98 \times 10^4\,\mathrm{s^{-1}}),$$
$$k_{MS} = 4.2 \times 10^4\,\mathrm{s^{-1}} \quad (5.5 \times 10^4\,\mathrm{s^{-1}},\ 6.3 \times 10^4\,\mathrm{s^{-1}}).$$

From the comparison of the two sets of data it is seen that the noise analysis is qualitatively consistent with the results of the different relaxation measurements. This is already apparent from the values of the two relaxation time constants of the voltage-jump experiment $\tau_1 = 6.5$ μs and $\tau_2 = 13.4$ μs which may be compared with $1/2\pi f_c = 16$ μs. The values of τ_1 and τ_2, which differ by only a factor of about two, also explain that, within the given resolution of the spectral analysis, only one dispersion process could be detected.

Furthermore from Table 1 it may be seen that the time constant $\tau_c = 1/2\pi f_c$ increases by about a factor of four when the fatty acid chain length is varied from C_{18} to C_{22}. This finding is in agreement with corresponding charge-pulse experiments (Benz *et al.*, 1977). In the latter case a change of the corresponding relaxation times $\tau_1(\tau_2)$ by a factor of about two (three) may be calculated from the measured values of k_R, k_D, k_S and k_{MS}.

Discussion

In this study we have shown that an ion-carrier system exhibits a characteristic current-noise spectrum which is different from other types of noise such as the familiar opening-closing current noise from ion channels. The current noise in the presence of valinomycin and Rb^+ has been measured under equilibrium conditions, i.e., with identical aqueous solutions on both sides of the membrane and at zero voltage. This has the advantage that kinetic information on the transport process can be obtained from a virtually unperturbed system. Furthermore, under equilibrium conditions the theoretical analysis can be based on Nyquist's theorem which relates the measured noise spectrum in a straightforward way to the elementary rate constants of the transport system.

The experimentally observed spectrum is frequency independent ("white") both at low and at high frequencies; this behavior is predicted by the theoretical model of carrier-mediated ion transport. The low-frequency limit is related to the steady-state conductance of the carrier system and the high-frequency limit to the initial conductance after a voltage jump. The transition-between these limiting values is characterized by two dispersions which correspond to the two time constants governing the voltage-jump relaxation behavior of the system (under certain conditions, as in the case of the valinomycin/Rb^+ experiments described here, the two dispersions may fuse into a single dispersion region).

In previous studies with ion carriers (Wanke, 1975; Szabo, 1977)

excess noise of the form described here could not be observed. The reason very probably is that the measurements have been carried out at rather low frequencies, whereas the characteristic dispersion regions occur at much higher frequencies. For instance, in the studies of the valinomycin/K^+ system on monoolein membranes (Szabo, 1977) a corner frequency above 30 kHz has to be expected from existing relaxation data (Knoll & Stark, 1975) which is outside the used experimental frequency range (10–1000 Hz).

It is interesting to compare the noise characteristic of the ion carrier with the noise of a similar but simpler ion transport system, namely, a bilayer doped with hydrophobic ions (Kolb & Läuger, 1977). In the experimental example studied previously (dipicrylamine in a phospholipid membrane), the exchange of hydrophobic ions between membrane and water is very slow so that the system behaves as if the ions were unable to leave the membrane and were bound to move back and forth across the central energy barrier in the membrane. The signal recorded in the external circuit then consists of a series of pulses originating from the translocation of single ions across the barrier. According to Carson's theorem a series of delta pulses leads to a white noise spectrum, provided that the pulses are uncorrelated. In the case of the hydrophobic ion, however, the pulses are correlated, because, if a single ion is regarded, a positive pulse is always followed by a negative pulse (and vice versa). This pulse correlation leads to a decline in the spectral intensity toward low frequencies, the corner frequency being approximately equal to the average frequency by which ions cross the barrier. Similar considerations also apply to the ion carrier, the main difference being that in this case ions are able to cross the interface by the processes of association and dissociation of the ion-carrier complex. The current pulses are then no longer strongly correlated and, accordingly, the spectrum becomes again white at low frequencies.

In biological membranes the most common type of noise which has been studied so far is the noise originating from the opening and closing of ion channels. This "channel noise" is a nonequilibrium noise characterized by a Lorentzian spectrum which is "white" and in excess of thermal noise at low frequencies and declines toward high frequencies. Apart from the completely different shape of the spectrum, the "transport noise" described here differs from "channel noise" in so far as current noise in the carrier system is observed even under equilibrium conditions, i.e., at zero net ion flux, whereas the spectral intensity of the opening-closing noise vanishes at zero current.

This work has been financially supported by the Deutsche Forschungsgemeinschaft (Sonderforschungsbereich 138).

Appendix A

Derivation of Eqs. (4)–(9)

We assume that a periodic voltage

$$u = u_0 \cos \omega t \tag{A1}$$

is applied to the membrane; ω is the angular frequency, t the time and u is equal to the membrane voltage V_m expressed in units of $kT/e_0 \approx 25\,\text{mV}$:

$$u = \frac{V_m}{kT/e_0}. \tag{A2}$$

In the following we restrict the analysis to small signals ($|u_0| \ll 1$). In this limit the voltage dependence of the translocation rate constant k_{MS} is approximately given by

$$k'_{MS} \approx k_{MS}(1 + u/2); \tag{A3}$$

$$k''_{MS} \approx k_{MS}(1 - u/2) \tag{A4}$$

(Läuger & Stark, 1970). k'_{MS} and k''_{MS} are the rate constants for jumps from left to right and from right to left, respectively (Fig. 1). The rate of change of the interfacial concentrations of free carrier S and complex MS^+ are given by

$$\frac{dN'_S}{dt} = k_D N'_{MS} - c_M k_R N'_S - k_S N'_S + k_S N''_S; \tag{A5}$$

$$\frac{dN''_S}{dt} = k_D N''_{MS} - c_M k_R N''_S - k_S N''_S + k_S N'_S; \tag{A6}$$

$$\frac{dN'_{MS}}{dt} = -k_D N'_{MS} + c_M k_R N'_S - k'_{MS} N'_{MS} + k''_{MS} N''_{MS}; \tag{A7}$$

$$\frac{dN''_{MS}}{dt} = -k_D N''_{MS} + c_M k_R N''_S - k''_{MS} N''_{MS} + k'_{MS} N'_{MS}. \tag{A8}$$

Introducing new variables:

$$r = N'_S + N''_S; \qquad s = N'_{MS} + N''_{MS} \tag{A9}$$

$$x_1 = N'_S - N''_S; \qquad x_2 = N'_{MS} - N''_{MS} \tag{A10}$$

one obtains from Eqs. (2), (A5) and (A6):

$$\frac{dr}{dt} = -(c_M k_R + k_D) r + k_D N. \tag{A11}$$

In the asymptotic limit ($t \to \infty$) Eq. (A11) has only the time-independent solution $dr/dt = 0$ ($c_M k_R, k_D$ and N are time independent); this gives

$$r = 2N_S = N \frac{k_D}{c_M k_R + k_D}. \tag{A12}$$

In a similar way one finds

$$s = 2N_{MS} = N \frac{c_M k_R}{c_M k_R + k_D}. \tag{A13}$$

(N_S and N_{MS} are the interfacial concentrations of S and MS^+ at equilibrium). Using Eqs. (A1), (A3), (A4), (A7), (A8) and (A10) and neglecting terms of the order of $u x_2$ one obtains

$$\frac{dx_1}{dt} = -(c_M k_R + 2k_S) x_1 + k_D x_2; \tag{A14}$$

$$\frac{dx_2}{dt} = c_M k_R x_1 - (k_D + 2k_{MS}) x_2 - k_{MS} s u_0 \cos \omega t. \tag{A15}$$

It is easily verified that this system of coupled differential equations is equivalent to

$$\frac{dy_1}{dt} = -\frac{1}{\tau_1} y_1 - p_{12} k_{MS} s u_0 \cos \omega t; \tag{A16}$$

$$\frac{dy_2}{dt} = -\frac{1}{\tau_2} y_2 - p_{22} k_{MS} s u_0 \cos \omega t \tag{A17}$$

by virtue of the following transformation:

$$\begin{aligned} y_1 &= p_{11} x_1 + p_{12} x_2; & x_1 &= q_{11} y_1 + q_{12} y_2; \\ y_2 &= p_{21} x_2 + p_{22} x_2; & x_2 &= q_{21} y_2 + q_{22} y_2; \end{aligned} \tag{A18}$$

$$\begin{aligned} p_{11} &= \frac{P + \sqrt{a}}{2k_D \sqrt{a}}; & q_{11} &= k_D; \\ p_{12} &= -1/2\sqrt{a}; & q_{12} &= -k_D; \end{aligned} \tag{A19}$$

$$p_{21}=\frac{P-\sqrt{a}}{2k_D\sqrt{a}}; \qquad q_{21}=P-\sqrt{a};$$

$$p_{22}=-1/2\sqrt{a}; \qquad q_{22}=-P-\sqrt{a};$$

$$P=\tfrac{1}{2}(c_M k_R-k_D+2k_S-2k_{MS}); \tag{A20}$$

$$Q=\tfrac{1}{2}(c_M k_R+k_D+2k_S+2k_{MS}); \tag{A21}$$

$$a=P^2+c_M k_R k_D; \tag{A22}$$

$$1/\tau_1=Q+\sqrt{a}; \qquad 1/\tau_2=Q-\sqrt{a}. \tag{A23}$$

In order to solve Eqs. (A16) and (A17), we introduce complex variables η_1 and η_2 with $\mathrm{Re}(\eta_1)=y_1$ and $\mathrm{Re}(\eta_2)=y_2$

$$\frac{d\eta_1}{dt}=-\frac{1}{\tau_1}\eta_1-p_{12}k_{MS}s u_0\exp(j\omega t); \tag{A24}$$

$$\frac{d\eta_2}{dt}=-\frac{1}{\tau_2}\eta_2-p_{22}k_{MS}s u_0\exp(j\omega t) \tag{A25}$$

(j is the imaginary unit). The solution of Eqs. (A24) and (A25) reads

$$\eta_1=-\tau_1\frac{1-j\omega\tau_1}{1+\omega^2\tau_1^2}p_{12}k_{MS}s u_0\exp(j\omega t); \tag{A26}$$

$$\eta_2=-\tau_2\frac{1-j\omega\tau_2}{1+\omega^2\tau_2^2}p_{22}k_{MS}s u_0\exp(j\omega t). \tag{A27}$$

The time-dependent current $I(t)$ which is measured in the external circuit is the sum of the charging current $C_m dV_m/dt$ (C_m is the membrane capacitance) and the current from the transport of MS^+ across the membrane:

$$I(t)=e_0 A_m(k'_{MS}N'_{MS}-k''_{MS}N''_{MS})+C_m\frac{dV_m}{dt}. \tag{A28}$$

A_m is the area of the membrane. Introducing Eqs. (A1)–(A4), (A9), (A10) and (A18) and neglecting terms of the order of ux_2, one obtains

$$I(t)=e_0 A_m k_{MS}\left(q_{21}y_1+q_{22}y_2+\frac{s}{2}u_0\cos\omega t\right)$$
$$-\frac{kT}{e_0}u_0 C_m\omega\cdot\sin\omega t. \tag{A29}$$

We now replace $I(t)$ by a complex current $J(t)$ with $\mathrm{Re}(J)=I$:

$$J(t)=e_0 A_m k_{MS}\left[q_{21}\eta_1+q_{22}\eta_2+\frac{s}{2}u_0\exp(j\omega t)\right]+\frac{kT}{e_0}u_0 C_m j\omega\cdot\exp(j\omega t). \tag{A30}$$

The complex admittance $Y(\omega)$ is defined in the following way: if a voltage

$$V_m(t)=V_{m0}\cos\omega t \tag{A31}$$

is applied to the membrane, the resulting current is given by

$$I(t)=I_0\cos(\omega t-\varphi); \tag{A32}$$

$$I_0=V_{m0}|Y(\omega)|=V_{m0}\sqrt{\mathrm{Re}^2[Y(\omega)]+Jm^2[Y(\omega)]}; \tag{A33}$$

$$tg\varphi=-\frac{Jm[Y(\omega)]}{\mathrm{Re}[Y(\omega)]} \tag{A34}$$

(Jm means "imaginary part of"). On the other hand, the complex current $J(t)$ is given by ($u_0=e_0 V_{m0}/kT$):

$$J(t)=Y(\omega)\,u_0\frac{kT}{e_0}\exp(j\omega t) \tag{A35}$$

(it is easily shown that this equation is equivalent to Eqs. (A31)–(A34) with $\mathrm{Re}(J)=I$).

Combination of Eqs. (A30) and (A35) gives, together with Eq. (A26) and (A27):

$$\mathrm{Re}[Y(\omega)]=\frac{e_0^2}{kT}A_m N_{MS} k_{MS}\left(1-\frac{\alpha_1}{1+\omega^2\tau_1^2}-\frac{\alpha_2}{1+\omega^2\tau_2^2}\right); \tag{A36}$$

$$\mathrm{Im}[Y(\omega)]=\omega C_m+\frac{e_0^2}{kT}A_m N_{MS} k_{MS}\left(\frac{\alpha_1\omega\tau_1}{1+\omega^2\tau_1^2}+\frac{\alpha_2\omega\tau_2}{1+\omega^2\tau_2^2}\right); \tag{A37}$$

$$\alpha_1=\frac{k_{MS}}{\sqrt{a}}\cdot\frac{\sqrt{a}-P}{\sqrt{a}+Q};\qquad \alpha_2=\frac{k_{MS}}{\sqrt{a}}\cdot\frac{P+\sqrt{a}}{Q-\sqrt{a}}. \tag{A38}$$

Introduction of Eq. (A36) into Eq. (3) then yields Eq. (4) for the spectral intensity of current noise.

Appendix B

Determination of the Model Parameters from the Spectral Data

Successive elimination of the rate constants and of N_{MS} from Eqs. (4)–(9) leads to the following expressions ($\lambda_1 \equiv 1/\tau_1$, $\lambda_2 \equiv 1/\tau_2$):

$$k_{MS} = \tfrac{1}{2}(\alpha_2 \lambda_2 - \alpha_1 \lambda_1); \tag{B1}$$

$$k_S = \frac{\lambda_1 \lambda_2 [4k_{MS}^2(\alpha_2 - \alpha_1 - 1) - \alpha_1 \alpha_2 (\lambda_1 - \lambda_2)^2]}{4k_{MS}(\alpha_1 \lambda_1^2 - \alpha_2 \lambda_2^2 + 4k_{MS}^2)}; \tag{B2}$$

$$k_R = \frac{\alpha_1 \alpha_2 \lambda_1 \lambda_2 (\lambda_1 - \lambda_2)^2}{2c_M k_{MS}(\alpha_1 \lambda_1^2 - \alpha_2 \lambda_2^2 + 4k_{MS}^2)}; \tag{B3}$$

$$k_D = \frac{\alpha_2 \lambda_2^2 - \alpha_1 \lambda_1^2 - 4k_{MS}^2}{2k_{MS}}; \tag{B4}$$

$$N_{MS} = \frac{S_I(\infty)}{4e_0^2 k_{MS}}. \tag{B5}$$

References

Benz, R. 1972. Kinetik des Carriertransportes durch bimolekulare Phospholipidmembranen. Thesis. University of Konstanz, Konstanz

Benz, R., Fröhlich, O., Läuger, P. 1977. Influence of membrane structure on the kinetics of carrier-mediated ion transport through lipid bilayers. *Biochim. Biophys. Acta* **46**:465

Benz, R., Fröhlich, O., Läuger, P., Montal, M. 1975. Electrical capacity of black lipid films and of lipid bilayers made of monolayers. *Biochim. Biophys. Acta* **394**:323

Benz, R., Läuger, P. 1976. Kinetic analysis of carrier-mediated ion transport by the charge-pulse technique. *J. Membrane Biol.* **27**:171

Benz, R., Stark, G., Janko, K., Läuger, P. 1973. Valinomycin-mediated ion transport through neutral lipid membranes: Influence of hydrocarbon chain length and temperature. *J. Membrane Biol.* **14**:339

Callen, H.B., Green, R.F. 1952. On a theorem of irreversible thermodynamics. *Phys. Rev.* **86**:702

Callen, H.B., Welton, T.A. 1951. Irreversibility and generalized noise. *Phys. Rev.* **83**:34

Conti, F., Wanke, E. 1975. Channel noise in nerve membranes and lipid bilayers. *Q. Rev. Biophys.* **8**:451

DeFelice, L.J. 1977. Fluctuation analysis in neurobiology. *Int. Rev. Neurobiol.* (*in press*)

Eisenman, G., Krasne, S., Ciani, S. 1975. The kinetic and equilibrium components of selective ionic permeability mediated by nactin- und valinomycin-type carriers having systematically varied degrees of methylation. *Ann. N.Y. Acad. Sci.* **264**:34

Feldberg, S.W., Nakadomari, H. 1977. Charge pulse studies of transport phenomena in bilayer membranes. II. Detailed theory of steady-state behavior and application to valinomycin-mediated potassium transport. *J. Membrane Biol.* **31**:81

Fishman, H.M., Dorset, D.L. 1973. Comments on electrical fluctuations associated with active transport. *Biophys. J.* **13**:1339

Hladky, S.B. 1975. Steady-state ion transport by nonactin and trinactin. *Biochim. Biophys. Acta* **375**:350

Knoll, W., Stark, G. 1975. An extended kinetic analysis of valinomycin-induced Rb-transport through monoglyceride membranes. *J. Membrane Biol.* **25**:249

Kolb, H.-A., Läuger, P. 1977. Electrical noise from lipid bilayer membranes in the presence of hydrophobic ions. *J. Membrane Biol.* **37**:321

Kubo, R. 1957. Statistical mechanical theory of irreversible processes. General theory and simple applications to magnetic and conduction processes. *J. Phys. Soc.* Jpn. **12**:570

Läuger, P., Lesslauer, W., Marti, E., Richter, J. 1967. Electrical properties of bimolecular phospholipid membranes. *Biochim. Biophys. Acta* **135**:20

Läuger, P., Stark, G. 1970. Kinetics of carrier-mediated ion transport across lipid bilayer membranes. *Biochim. Biophys. Acta* **211**:458

Neher, E., Stevens, C.F. 1977. Conductance fluctuations and ionic pores in membranes. *Ann. Rev. Biophys. Bioeng.* **6**:345

Nyquist, H. 1928. Thermal agitation of electric charge in conductors. *Phys. Rev.* **32**:110

Poussart, D.J.M. 1971. Membrane current noise in lobster axon under voltage clamp. *Biophys. J.* **11**:211

Segal, J.R. 1972. Electrical fluctuations associated with active transport. *Biophys. J.* **12**:1371

Segal, J.R. 1973. *Reply to:* Comments on electrical fluctuations associated with active transport. *Biophys. J.* **14**:513

Stark, G., Benz, R. 1971. The transport of potassium through lipid bilayer membranes by the neutral carriers valinomycin and monactin. Experimental studies to a previously proposed model. *J. Membrane Biol.* **5**:133

Stark, G., Benz, R., Pohl, G., Janko, K. 1972. Valinomycin as a probe for the study of structural changes of black lipid membranes. *Biochim. Biophys. Acta* **266**:603

Stark, G., Ketterer, B., Benz, R., Läuger, P. 1971. The rate constants of valinomycin-mediated ion transport through thin lipid membranes. *Biophys. J.* **11**:981

Szabo, G. 1977. Electrical characteristics of ion transport in lipid bilayer membranes. *Ann. N.Y. Acad. Sci. (in press)*

Szabo, G., Eisenman, G., Laprade, R., Ciani, S.M., Krasne, S. 1973. Experimentally observed effects of carriers on the electrical properties of bilayer membranes-Equilibrium domain. *In:* Membranes – A Series of Advances. G. Eisenman, editor, Vol. II, pp. 179–328. M. Dekker, New York

Verveen, A.A., DeFelice, L.J. 1974. Membrane noise. *Prog. Biophys. Mol. Biol.* **28**:189

Wanke, E. 1975. Monazomycin and nystatin channel noise. *5th Int. Biophys. Congr. Abstr. P*-368, 112